



Lavery, M.J.P., Speirits, F.C., Barnett, S.M., and Padgett, M.J. (2013)  
Detection of a spinning object using light's orbital angular momentum.  
Science, 341 (6145). pp. 537-540. ISSN 0036-8075

Copyright © 2013 American Association for the Advancement of Science.

A copy can be downloaded for personal non-commercial research or  
study, without prior permission or charge

The content must not be changed in any way or reproduced in any format  
or medium without the formal permission of the copyright holder(s)

When referring to this work, full bibliographic details must be given

<http://eprints.gla.ac.uk/85025/>

Deposited on: 10 Jan 2014

Enlighten – Research publications by members of the University of Glasgow  
<http://eprints.gla.ac.uk>

# Detection of a spinning object using light's orbital angular momentum

Martin P. J. Lavery<sup>1</sup>, Fiona C. Speirits<sup>2</sup>, Stephen M. Barnett<sup>2</sup> and Miles J. Padgett<sup>1</sup>

<sup>1</sup> School of Physics and Astronomy, SUPA, University of Glasgow, Glasgow G12 8QQ, UK

<sup>2</sup> Department of Physics, SUPA, University of Strathclyde, Glasgow G4 0NG, UK

**The linear Doppler shift is widely used to infer the velocity of approaching objects, but this shift does not detect rotation. By analysing the orbital angular momentum of the light scattered from a spinning object we observe a frequency shift many times greater than the rotation rate. This rotational frequency shift is still present when the angular momentum vector is parallel to the observation direction. The multiplicative enhancement of the frequency shift may have applications in both terrestrial and astronomical settings for the remote detection of rotating bodies.**

The spin angular momentum of light is manifested as circular polarisation and corresponds to the  $\hbar$  spin angular momentum of the photon. It was recognised that light beams with a helical phase structure described by  $\exp(i\ell\phi)$  also carry an orbital angular momentum corresponding to  $\ell\hbar$  per photon [1]. Over the last 20 years, this orbital angular momentum has been studied in various contexts ranging from optical micromanipulation to quantum optics [2].

Consideration has been given to the use of orbital angular momentum in imaging and remote sensing, where the detection of the angular momentum may reveal the structure or potentially the motion of the object [3-7]. When light is scattered from a spinning object we find that the rotation rate of the object can be measured by analysing frequency shifts in the orbital angular momentum of the light. This new method of remote sensing has applications in both terrestrial and astronomical arenas.

The Doppler shift is a well-known phenomenon, where the relative velocity  $v$  between light source and observer gives a frequency shift  $\Delta f$ . The resulting frequency shift is  $\Delta f = f_0 v/c$ , where  $f_0$  is the unshifted frequency and  $c$  is the speed of light. Less well-known than this linear effect is the rotational, or angular, Doppler effect [8-11]. For a beam with helical phase-fronts, a rotation of angular frequency  $\Omega$  between the source and observer shifts the frequency by

$$\Delta f = (\ell + \sigma) \Omega / 2\pi, \quad (1)$$

where  $\sigma = \pm 1$  for right- and left-handed circularly polarised light and 0 for linearly polarised light, and hence  $(\ell + \sigma)\hbar$  is the total angular momentum per photon [12].

All of this previous rotational work has been based on pure OAM states, explicitly rotated using specialist optical elements.

The standard linear Doppler shift applies when the relative motion between source and observer is along the direction of observation. For motion transverse to the direction of observation, a reduced Doppler shift can still be observed in the light scattered at an angle  $\alpha$  from the surface normal. For small values of  $\alpha$ , this reduced Doppler shift is given by

$$\Delta f = \alpha \times f_0 v/c. \quad (2)$$

Key to this frequency shift is the fact that the form of the scattered light is not determined solely by the laws of reflection. The roughness of the surface means that some of the light normally incident on the surface is scattered at angle  $\alpha$ .

The observation of this frequency shift in light scattered from a moving object is the basis of speckle, or laser Doppler, velocimetry, and it is used for the remote sensing of the transverse velocity of moving surfaces [13] or fluids [14]. (Fig. 1A).

It is also possible to understand speckle velocimetry in the time domain. In illumination mode, the resulting interference between the two beams at  $\pm\alpha$  creates straight-line fringes with period  $\Lambda = \lambda/\sin 2\alpha$ . When a rough surface translates across this fringe pattern the inhomogeneity of the surface results in a slight modulation in the intensity of the scattered light. The frequency of this modulation is  $f_{mod} = v/\Lambda$ , which is exactly the same rate as anticipated from the differential Doppler shifts of the two beams given by eqn. 2. The depth of the modulation depends upon the period of the fringes compared to the period of the surface roughness, where the depth is maximised when the two periods match. These two complimentary explanations of speckle velocimetry have an angular equivalent.

In a helically-phased beam, the Poynting vector, and hence the optical momentum, has an azimuthal component at every position within the beam. The angle between the Poynting vector and the beam axis is  $\alpha = \ell\lambda/2\pi r$ , where  $r$  is the radius from the beam axis [15] (Fig. 1B). In the frequency domain, for a helically-phased beam illuminating a spinning object, we can see from eqn. 2 that the Doppler frequency shift of the on-axis scattered light is given as

$$\Delta f = \frac{\ell\lambda}{2\pi r} \times f_0 \frac{\Omega r}{c} = \frac{\ell\Omega}{2\pi}, \quad (3)$$

Note also in eqn. 3 there is no dependence upon polarisation since, even after scattering, the polarisation state of the light is largely unchanged.

When the illumination comprises two helically-phased beams of opposite values of  $\ell$ , their scattering into a common detection mode gives an intensity modulation of frequency

$$f_{mod} = 2|\ell|\Omega/2\pi. \quad (4)$$

Even, if the detection is multi-modal, each of the modes experiences the same frequency shift.

Within the time domain the interpretation is that the superposition of two helically-phased beams with opposite values of  $\ell$  creates a beam cross-section with a modulated intensity of  $2\ell$  radial petals [16]. Therefore, the light scattered from the rough surface of a spinning disc will undergo an intensity modulation also given by equation (4)

Linear optical systems tend to be reciprocal in that the source and detector can be interchanged. Consequently, we would expect the frequency shift, produce by the spinning surface, to be observed either in the case of illumination by a beam containing OAM and the on-axis detection of scattered light or for on-axis illumination and detection of an OAM component in the scattered light.

For illumination of the spinning object with light of specific OAM modes a diode laser at 670 nm is coupled to a single-mode fibre, the output of which is collimated and used to illuminate a phase-only spatial light modulator (SLM). The SLM is programmed with a kinoform to produce a superposition of two helically-phased beams with opposite signs of  $\ell$ . The phase contrast is adjusted over the SLM cross-section such that the radial intensity structure of the diffracted beam is a single annulus corresponding to a  $p = 0$  Laguerre-Gaussian mode [17]. The plane of the SLM is reimaged using an afocal telescope to illuminate the spinning object. Relay mirrors allow the axis of the illuminating beam to be precisely aligned to the rotation axis of the object. The diameter of the beam superposition on the object is approximately 18 mm, which gives a petal period of approximately 2 mm for typical values of  $\ell = \pm 18$ . This petal beam illuminates a metallic surface attached to a plastic rotor, which is driven at speeds ranging from 200 – 500 radians per second. The rough nature of the surface means that no matter what the modal composition of the illumination light, the light scattered from the surface covers a very wide range of modes. The modal bandwidth of this scattered light is a function of both the size of the illuminating beam and the range of angles over which the light is scattered or, more importantly, detected. The bandwidth is usefully approximated in terms of Fresnel number of the optical system. A lens and a large area photodiode are used to collect light scattered from the spinning surface. The output of the detector is digitised and Fourier-transformed to give the frequency components of the detected intensity modulation(see supplementary information).

For the light scattered from the rotating surface when illuminated with a Laguerre-Gaussian superposition of  $\ell = \pm 18$  (Fig. 2B), the resulting power spectra were obtained from a data collection period of 1 second. A clearly distinguishable peak was observed at a frequency matching that predicted by eqn. 4. To further test the relationship predicted in eqn. 4, the rotation speed and value of  $|\ell|$  were varied and compared to the results expected from the prediction, (Fig. 2C). The subsidiary peaks at higher frequencies arise from a cross-coupling to different mode indices corresponding to  $\Delta\ell = 37, \Delta\ell = 38$  etc. As adjacent peaks correspond to  $\Delta\ell = \pm 1$ , they are separated, in frequency, from each other by the rotation speed  $\Omega$ . Most

likely is that this cross-coupling arises from a slight misalignment in the experiment between the rotation and detection axes [18,19].

It is interesting to note that the relative frequency shift of the +ve and -ve orbital angular momentum components gives an energy imbalance between the states, yet not necessarily a change in their angular momentum. The latter depends solely upon photon number in each mode, slight changes in which would not be observable in this experiment. Indeed, although the scattered light contains many modes, irrespective of the detailed mode spectrum we would not expect it to be changed by the rotation of the surface. We note that for an individual mode, the  $\ell$ -fold rotational symmetry remains  $\ell$ -fold symmetric even in a rotating frame.

The underlying mechanism introducing this frequency shift can be understood either with respect to the laboratory or the rotating frame. In the laboratory frame, the change in local ray direction,  $\alpha$ , between the incident and detected light means there is an azimuthal reaction force acting on the scattering surface. Doing work against this force is the energy input required to shift the frequency of the light, not dissimilar in origin to the mechanism associated with the rotation of a mode converter [20]. The +ve and -ve OAM components undergo up- and down-shifts in frequency, which interfere to give the modulation in intensity recorded at the detector. In the rotating frame, the incident beams are themselves seen as rotating and hence are subject to a rotational Doppler shift, with the +ve and -ve OAM components again experiencing up- and down-shifts respectively. Scattering centres on the surface radiate both of the frequencies back to the detector, where they again interfere to give the observed modulation in intensity.

The equivalent interpretation in terms of a Doppler shift or patterned projection applies both to OAM illumination and OAM detection. Consequently, it is possible to interchange the laser and detector. In this alternative configuration, the spinning object is illuminated directly with the expanded laser beam. Some of the scattered light is incident on the SLM, which is programmed with an identical kinoform as previously, to couple a superposition of  $\pm\ell$  into the single-mode fibre. The SLM and the fibre are now acting as a mode filter to select only the desired superposition from the many modes within the scattered light. The power of light in these desired modes is a small fraction of that illuminating the object, so the light transmitted through the fibre is only of low intensity. We measure the light transmitted through the fibre using a photomultiplier, the output from which is Fourier-transformed as in the previous configuration. To enhance the signal, the metal surface was lightly embossed with a pattern of 18-fold rotational symmetry, resulting in a dominant overlap with the modal superposition of  $\ell = \pm 18$  ( $\Delta\ell = 36$ ).

Figure 3 shows the frequency spectrum of the intensity modulation in the detected light as obtained over a data collection period of 5 minutes. Again the frequency of this peak can be predicted by eqn. 4 to reveal the rotational speed of the object.

We have shown that an orbital angular momentum-based analysis of the scattered light makes it possible to infer the rotation speed of a distant object, even though the

rotation axis is parallel to the observation direction. The high mode number of the orbital angular momentum state, and the resulting rotational symmetry, means that the recorded frequency is a factor of  $2\ell$  higher than the rotation frequency itself. A similar advantage in using OAM has been noted previously for fixed angle measurement in both classical [21] and quantum [22] regimes. Of course, the maximum value of OAM mode that can be used is set by the modal bandwidth of the scattered light. However, increasing the bandwidth also reduces the fraction of the scattered light that falls within the scattered mode. Consequently, the degree of OAM enhancement of the rotation detection is a complicated function of the experimental conditions.

Although the Doppler shift, Doppler velocimetry and their application to the remote measurement of transverse velocity are well known, this present work recognises that these phenomena have an angular equivalent. An analysis in terms of the orbital angular momentum gives a clear and intuitive understanding of the angular case. This understanding indicates possible applications in multiple regimes. Two application areas of particular promise are the potential for the remote sensing of turbulence in back-scattered light and the possible application to astronomy for the remote detection of rotating bodies.

- [1] L. Allen, M. W. Beijersbergen, R. J. C. Spreeuw, and J. P. Woerdman, *Phys Rev A* **45**, 8185 (1992).
- [2] A. M. Yao and M. J. Padgett, *Adv. Opt. Photon.* **3**, 161 (2011).
- [3] M. Harwit, *The Astrophysical Journal* **597**, 1266 (2003).
- [4] L. Torner, J. P. Torres, and S. Carrasco, *Opt Express* **13**, 873 (2005).
- [5] S. Fürhapter, A. Jesacher, S. Bernet, and M. Ritsch-Marte, *Opt Express* **13**, 689 (2005).
- [6] F. Tamburini, B. Thidé, G. Molina-Terriza, and G. Anzolin, *Nat Phys* **7**, 195 (2011).
- [7] G. Swartzlander, E. Ford, R. Abdul-Malik, L. Close, M. Peters, D. Palacios, and D. Wilson, *Opt Express* **16**, 10200 (2008).
- [8] B. A. Garetz, *J Opt Soc Am* **71**, 609 (1981).
- [9] I. Bialynicki-Birula and Z. Bialynicka-Birula, *Phys Rev Lett* **78**, 2539 (1997).
- [10] J. Courtial, K. Dholakia, D. A. Robertson, L. Allen, and M. J. Padgett, *Phys Rev Lett* **80**, 3217 (1998).
- [11] S. Barreiro, J. Tabosa, H. Failache, and A. Lezama, *Phys Rev Lett* **97**, 113601 (2006).
- [12] J. Courtial, D. A. Robertson, K. Dholakia, L. Allen, and M. J. Padgett, *Phys Rev Lett* **81**, 4828 (1998).
- [13] T. Asakura and N. Takai, *Appl. Phys.* **25**, 179 (1981).
- [14] R. Meynart, *Appl Optics* **22**, 535 (1983).
- [15] J. Leach, S. Keen, M. J. Padgett, C. D. Saunter, and G. D. Love, *Opt Express* **14**, 11919 (2006).
- [16] S. Franke-Arnold, J. Leach, M. J. Padgett, V. E. Lembessis, D. Ellinas, A. J. Wright, J. M. Girkin, P. Ohberg, and A. S. Arnold, *Opt Express* **15**, 8619 (2007).
- [17] J. Leach, M. R. Dennis, J. Courtial, and M. J. Padgett, *New J Phys* **7**, 55 (2005).

- [18] M. V. Vasnetsov, V. A. Pas'ko, and M. S. Soskin, *New J Phys* **7**, 46 (2005).
- [19] M. P. J. Lavery, G. C. G. Berkhout, J. Courtial, and M. J. Padgett, *J Opt* **13**, 064006 (2011).
- [20] M. J. Padgett, *J Opt A* **6**, S263 (2004).
- [21] S. M. Barnett and R. Zambrini, *J Mod Optic* **53**, 613 (2006).
- [22] R. Fickler, R. Lapkiewicz, W. N. Plick, M. Krenn, C. Schaeff, S. Ramelow, and A. Zeilinger, *Science* **338**, 640 (2012).

We thank EPSRC and DARPA InPho programme through the US Army Research Office award W911NF-10-1-0395 for financial support. SMB and MJP thank the Royal Society and Wolfson Foundation.

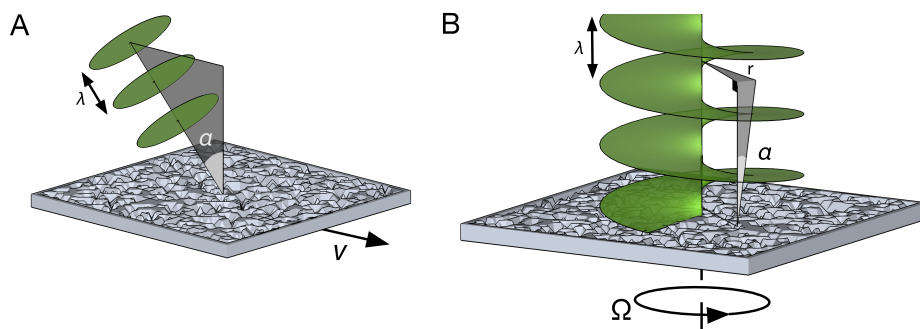


Fig. 1 The light scattered from a moving surface can be Doppler shifted in frequency. This frequency shift can be observed for (A) translation and, (B) rotation.

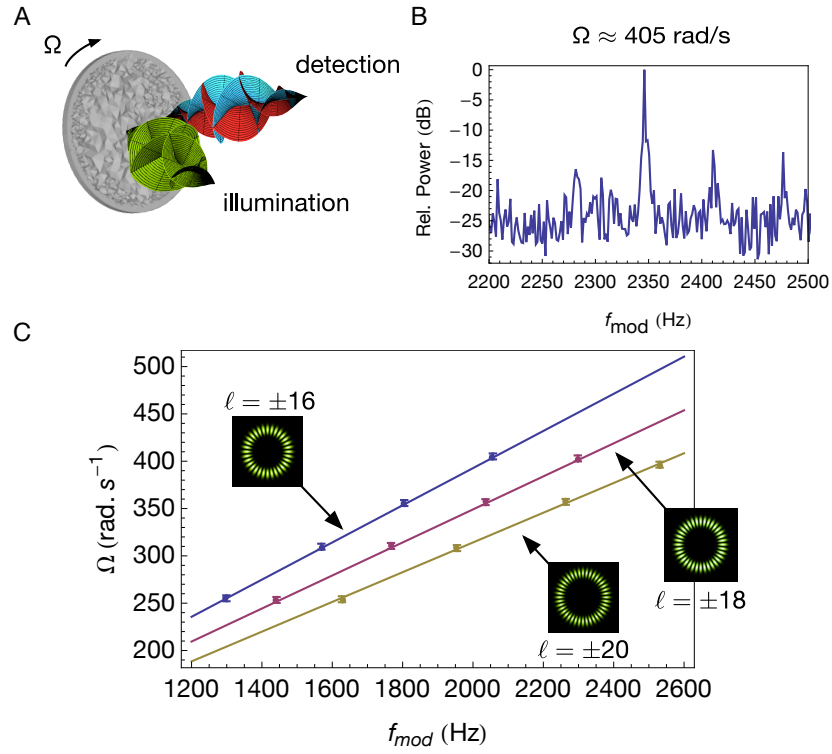


Fig. 2. (A) A superposition of helically-phased beams with opposite signs of  $\ell$ , incident on a surface rotating at a speed  $\Omega$ , results in a Doppler shift of the on-axis scattered light. The size of this shift is dependant on the value and sign of  $\ell$ . For a given input superposition, shown in green, the light scattered from the positive  $\ell$  beam will be blue-shifted and that from the negative  $\ell$  beam will be red-shifted. (B) This differential shift will result in an intensity modulation at a particular frequency,  $f_{mod} = 2346 \pm 1$  Hz. (C) values of  $f_{mod}$  were measured for different rotation speeds and values of  $|\ell|$ , shown as points, and were compared to the values predicted from eqn. 4, shown as solid lines.



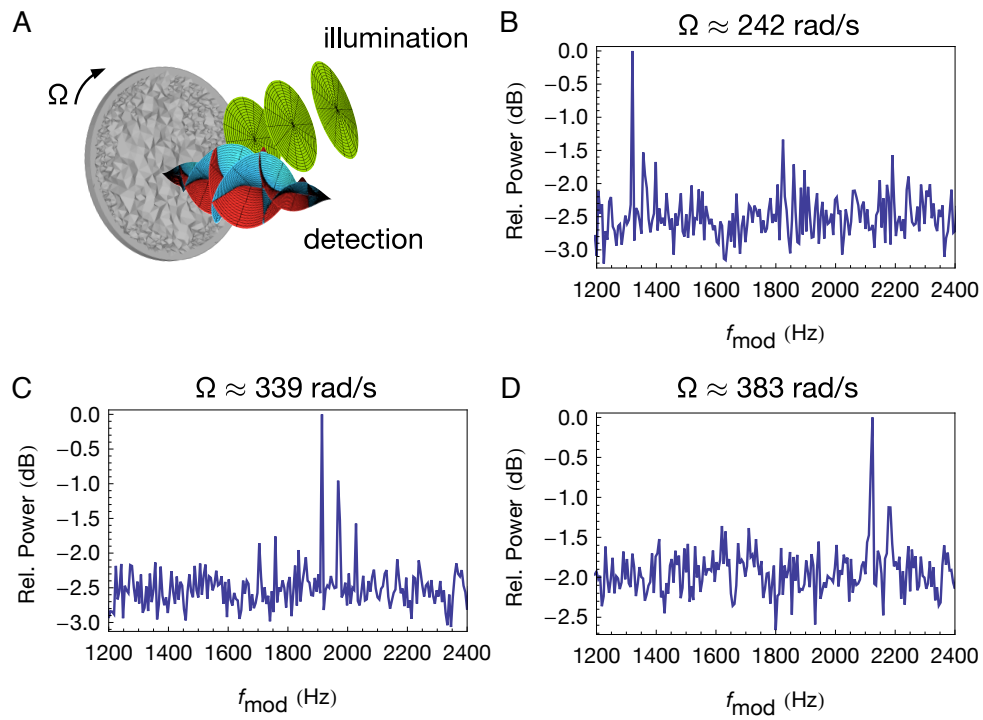


Fig. 3. (A) Light scattered from a uniformly illuminated spinning surface can be filtered to contain only specified modal components  $\ell = \pm 18$ . When these components are interfered, an intensity modulation is observed. Three different rotation speeds were of 242, 339 and 383 radians per second are presented (B-D) respectively, where corresponding beat frequencies of  $1320 \pm 20$  Hz,  $1914 \pm 21$  Hz and  $2124 \pm 30$  Hz were observed.